MODELING OF THERMAL AND GAS-DYNAMICAL PROCESSES IN CONTAINERS FOR STORAGE WEAPONS-GRADE PLUTONIUM

Alexander V. Voronkov, Evgenii A. Zemskov, Elena P. Sychugova and Alexander G. Churbanov

The Keldysh Institute of Applied Mathematics, Russian Academy of Sciences
4 Miusskaya Square, Moscow 125047, Russia
voron@kiam.ru

ABSTRACT

One of actual computing problems arising in connection with a problem of organization of storage of weapon plutonium is considered in this work. It is a problem of calculation of the temperature fields in containers and storage building in conditions of long-term storage of ingots of the weapon plutonium. The special technique taking into account peculiarities of the considered physical processes is developed for numerical modeling of thermal processes in containers including heat transfer on account of heat conduction, internal free convection, heat transfer by radiation. The efficiency of this technique in problems of calculation of temperature fields of containers with plutonium is shown on the example of calculation of some models of two cans container configurations designed in Westinghouse Savannah River Company and container AT400R. The different effects are analyzed by means of numerical modeling. These effects are connected with the accounting of natural convections of air in cavities of container, the accounting of flow of heat through a bottom of container to the rack of storage, the influence of gap between a bottom of container and rack of storage on distribution of temperatures.

1. INTRODUCTION

In the countries employing nuclear power there is observed essential exceeding of the processed plutonium over the volume of its usage. This fact becomes more impressive due to releasing of weapon plutonium declared by Russia and USA [1]. One of the most important engineering problems connected with safe storage of weapon plutonium in special containers located in storage rooms is an analysis of thermal conditions for metallic Pu and organic materials used in container construction. The plutonium oxidation rate as well as degradation

rate for plastic materials essentially depends on the temperature value. Both these processes at definite conditions can result in destruction of the container, formation and emission of radioactive aerosols containing plutonium oxides.

Many studies [2-6] deal with description of algorithms and calculations of the temperature in container elements at different variations of external parameters including the accidental ones as well as at the conditions of long-term storage in storage rooms. As a rule, in these calculations requiring coupled accounting of thermal conductivity, convection and radiation there are employed techniques allowing to simplify the general problem by means of its decomposition into subproblems and usage of effective thermal conductivity or resistance. In this work there is presented a numerical technique for the coupled computation of heat transfer via thermal conductivity, internal free convection and radiation. It is based on the heat conduction equation coupled with gas dynamic equations in order to take into account free convection in gas media.

2. DEVELOPMENT OF THE 2D AND 3D NUMERICAL ALGORITHMS FOR SIMULATION OF HEAT AND MASS TRANSFER PROCESSES IN CONTAINER

Convective heat and mass transfer processes occurring at fires and other types of combustion are characterized by slow enough flows of a gas mixture but by large density variations because of high temperature drops and essential modification of its composition due to proceeding chemical transformations [7, 8]. The traditional methods for solving problems of gas dynamics or incompressible fluids are unacceptable for calculation of this class of flows. It is necessary to develop special algorithms based on adequate mathematical models that take into account specific peculiarities of the considering physical processes characterized by the presence of a small parameter (low Mach number). Peculiarities of gas flows at low Mach numbers consist in the facts, that these flows, on the one hand, are similar to flows of a fluid - the propagation speed of small perturbation for them is much higher in compare with the gas velocity. On the other hand, the property of compressibility of medium is essential in gas flows and is not caused by the pressure influence (it means that the flow is characterized by small relative pressure variations about some average value). The essential difficulties are arisen in numerical simulation of flows of a viscous compressible gas on the basis of the full Navier-Stokes equations at low Mach numbers ($M < 0.01$). Nowadays difficulties of numerical calculation of these gas flows are well known but they are overcome by using the reduced models. The LMN-equations represent the reduced Navier-Stokes equations for a gas derived in assumption of a small value of the Mach number. A brief discussion of these models is given below.

2.1 LMN-APPROXIMATIONS

Historically appearing of LMN-approximations is connected with the solution of the important applied problems on flows of chemically reacting gas mixtures with strong heat

production. The detailed description of these models and methods of their derivation may be found, for example, in [9-12]. They were successfully employed for the solution of different applied problems including 3D simulation of fires in rooms.

The LMN-equations represent the reduced Navier-Stokes equations for a gas in the assumption of a small value of the Mach number. One of the ways for deriving the LMN-approximation is expansion of unknown functions into a series with respect to the small parameter $\gamma \mathrm{M}^2$. Then, after the substitution of these series into the full Navier-Stokes equations, we omit the equation terms of M^2 magnitude and higher. As the result the following system of LMN-equations are obtained:

$$\begin{aligned}
&\frac{\partial \rho}{\partial t} + div\rho\mathbf{v} = 0, \\
&\frac{\partial \rho v_i}{\partial t} + div\rho\, v_i\mathbf{v} + \nabla_i p_d = \frac{2}{\mathrm{Re}}\left(div_i \mu\dot{S} - \frac{1}{3}\nabla_i \mu div\mathbf{v} \right), \\
&\frac{\partial \rho T}{\partial t} + div\rho\mathbf{v}T = div\left(\frac{\lambda}{\mathrm{Re}\cdot \mathrm{Pr}}\nabla T \right) + \frac{\gamma - 1}{\gamma}\frac{\partial \overline{p}}{\partial t}, \quad \overline{p} = \rho T.
\end{aligned} \tag{1}$$

In the result of these simplifications the system of equations takes the form very similar to the incompressible Navier-Stokes equations. Due to the fact that instead of the pressure we have two new unknowns $\overline{p}\,(t)$ and $p_d(t,x)$, it is necessary to add one more equation in order to obtain a complete system of equations. Such the closing of the system is carried out via various ways in different works depending on the particular formulation of the problem. For flows in cavities with variation of the volume or mean temperature the system of LMN-equations is closed using the integral equation for the mean pressure. If it is a priori known that the mean pressure is fixed and equals some value P_0, then equation $\overline{p}(t) = P_0$ is used.

2.2 PECULIARITIES OF SOLVING THE FULL NAVIER-STOKES EQUATIONS AT LOW MACH NUMBER

First of all, it should be noted that for prediction of subsonic flows implicit methods are employed, as the rule. The explicit schemes are inefficient due to the Courant-Friedrichs-Levi restriction on the time-step. The permissible time-step for the explicit schemes is proportional to the Mach number. This restriction becomes very strong when the Mach number tends to zero.

However, usage of the implicit schemes for predicting gas flows at low Mach number does not lead automatically to success. If an algorithm does not take into account specific behavior of the pressure at low Mach numbers then at $\mathrm{M} < 0.01$ essential decreasing of accuracy and convergence rate is observed in some problems.

At $M \to 0$ the reference value of the mean pressure P_0 becomes much higher than the reference value $\rho_0 V_0^2$ for pressure fluctuations about mean pressure P_0. The velocity field depending on the pressure gradient is defined by these fluctuations of the pressure about its average value. If the standard representation of the pressure is used where the above mentioned peculiarities do not take into account then the usual normalization $P = P_0 p$ leads to appearing the factor $1/M^2$ at term *grad p* in the momentum equation. During the calculation of p the round-off errors will be divided by M^2. As the sequence, at $M \to 0$ accuracy of both explicit and implicit algorithms will decrease whereas the computational cost will increase. The developed equivalent formulation of the full (without any reductions) Navier-Stokes equations that do not contain a singularity of type $1/M^2$ is considered below.

2.3 REGULARIZATION OF THE NAVIER-STOKES EQUATIONS

Let us consider the pressure as the sum of average pressure $\overline{p}(t)$ and dynamic part $p_d(t,x)$:

$$P(t,x) = P_0 \overline{p}(t) + \rho_0 V_0^2 p_d(t,x). \tag{2}$$

The dimensionless pressure can be represented like this:

$$p(t,x) = \overline{p}(t) + \gamma M^2 p_d(t,x). \tag{3}$$

At normalization we take into account that the average pressure and dynamic pressure have different reference values. The representation of the pressure as the sum of two terms with twofold normalization allows obtaining such a form of the full Navier-Stokes equations where there are no singularities of M^{-2} type. In the pressure representation (3) instead of single unknown $p(t,x)$ we introduce two others, namely, $\overline{p}(t)$ and $p_d(t,x)$. So, to close the system of equations, we use the integral relation defining volume-averaged pressure $\overline{p}(t)$:

$$\overline{p} = \frac{1}{V_\Omega} \int_\Omega p d^3x, \quad V_\Omega = \int_\Omega d^3x. \tag{4}$$

Let us present the full system of the Navier-Stokes equations by taking into account the relation (2). For transition to dimensionless variables the standard normalization is used:

$$\begin{aligned} &t' = (V_0 / L_0)t, \quad x_i' = x_i / L_0, \quad v_i' = v_i / V_0; \quad i = 1,2,3; \quad p_d' = \left(P(t,x) - P_0 \overline{p}(t)\right) / \left(\rho_0 V_0^2\right), \\ &\rho' = \rho / \rho_0, \quad T' = T / T_0, \quad \lambda' = \lambda / \lambda_0, \quad \mu' = \mu / \mu_0, \quad C_p' = C_p / C_{p0}. \end{aligned} \tag{5}$$

Using relations (5), let us rewrite the full (without any reductions) Navier-Stokes equations in the dimensionless form:

$$\frac{\partial \rho}{\partial t} + div\rho\mathbf{v} = 0,$$
$$\frac{\partial \rho v_i}{\partial t} + div\rho v_i\mathbf{v} + \nabla_i p_d = \frac{2}{\mathrm{Re}}\left(div_i \mu\dot{S} - \frac{1}{3}\nabla_i \mu div\mathbf{v} \right) + F_i, \quad \mathbf{F} = \rho\mathbf{e}/Fr, \tag{6}$$
$$\frac{\partial \rho T}{\partial t} + div\rho\mathbf{v}T = div\left(\frac{\lambda}{\mathrm{Re}\cdot \mathrm{Pr}}\nabla T \right) + \frac{\gamma - 1}{\gamma}\left(\frac{\partial \overline{p}}{\partial t} + \gamma M^2 \left(\frac{\partial p_d}{\partial t} + \mathbf{v}\nabla p_d + \frac{J_{dis}}{\mathrm{Re}} \right) \right), \quad p = \rho T.$$

Here **e** – the unit vector defining the direction of the gravitational force.

Dimensionless criteria – the Mach, Reynolds, Prandtl and Froud numbers – are defined via reference values in (5). It should be noted that the average pressure $\overline{p}$ disappears from all terms with the pressure containing spatial derivatives. Moreover, in these equations there are no singularities of M^{-2} type that makes possible to do the passage to the limit $M \to 0$ in these equations. At M = 0 the system of equations (6) takes the form employed in LMN-models. The equation of state transforms into the form $\rho(t,x) = \overline{p}(t)/T(t,x)$, whereas in the energy equation the terms will disappear which are omitted at derivation of LMN-models.

2.4 NUMERICAL ALGORITHM

The operator-splitting technique that, in general, is very close to the well-known method SIMPLER [13] will be used. Let us consider the approximation in time. The continuity equation is approximated in the fully implicit fashion. In the temperature equation all terms containing the temperature are approximated implicitly. For efficient advancement in time we use the operator-splitting scheme of the Douglas-Rachford type for approximation of the momentum equation. It allows solving separately discrete problems for the velocity and pressure at every time level.

It should be noted that the processes of convective heat and mass transfer occurring at fires should be considered taking into account the complicated geometries of the real constructions. It is assumed to employ the developed early homogeneous algorithm [14], which indicated good features for the numerical implementation of the proposed algorithm above for predicting the slightly compressible reacting flows in arbitrary domains. It provides the following possibilities. A calculation domain can include:
(a) regions with flows of viscous heat-conducting compressible or incompressible medium;
(b) anisotropic porous media;
(c) solid heat-conducting bodies of complex form;
(d) internal partitions of zero thickness.

In flow regions the heat and mass transfer is governed by the Navier-Stokes equations for a compressible or incompressible fluid supplemented with the energy conservation equation. Heat transfer in solid bodies is described by the heat conduction equation. Heat transfer is calculated by the homogeneous way simultaneously in the whole domain (including flow

regions, porous media, solid bodies and partitions), i.e. the problem of conjugate heat transfer is solved. This algorithm has been implemented in code LMN2D.

3. NUMERICAL RESULTS

Using the developed code LMN2D there were conducted 2D predictions of thermal regimes of containers for plutonium storage – some configurations of the container designed in Westinghouse Savannah River Company [2] and container AT400R [3].

3.1 CALCULATION OF THE CONTAINER OF WESTINGHOUSE SAVANNAH RIVER COMPANY

To analyze accuracy and efficiency of the developed algorithm, there were conducted predictions of containers designed in Westinghouse Savannah River Company [2] and a comparative study of the derived numerical results has been done.

The first considered container # 1 consisted of two steel embedded cylinders. The external cylinder had sizes 0.108 x 0.1238 m whereas the internal one of smaller sizes contains the cylinder with plutonium about 2.2 kg with dimensions 0.053 x 0.053 m located at its bottom where heat generation with power 1 W takes place. On the left boundary of this calculation domain being the symmetry axis there are imposed the conditions of symmetry, the lower boundary is adiabatic, and on the upper and right boundaries there is specified the heat transfer into the environment having temperature 300 K with heat exchange coefficient of 1.5 W /(m^2 K). The calculations were conducted on a fine nonuniform grid of 163x297 points. The initial temperature in the whole domain was equal to T = 300 K. The prescribed constant heat generation in plutonium with power 1 W resulted in gradual heating of the whole container.

In work [2] there were considered and some other configurations connected with real situations in storage of containers with weapon plutonium located in a storage room. In particular, steady-state thermal regimes have been calculated for two other configurations – in the presence of the air gap between the container bottom and the storage rack and at its absence. In both cases it was taken into account that the container was located on a well-heatconducting steel storage rack. It should be noted that in work [2] a pure heat conduction problem has been considered with an effective anisotropic heat conductivity for air. In our predictions of similar containers we took into account free convection of air both in large gaps and in the small gap under the container bottom.

Using code LMN2D there was calculated container # 2 – the two can container with plutonium and internal heat-generation 10.35 W. In our predictions at the upper, lower and right boundaries of the domain there was specified heat transfer into environment with temperature and heat exchange coefficient 10.0 W/(m^2 K). The symmetry condition was

prescribed on the left boundary (the symmetry axis). Calculations were done using fine nonuniform grid of 145 x 222 points. The averaged temperatures obtained from our predictions for character surfaces of the container and storage rack are presented in Table I for all three calculated configurations. Results from [2] are also shown for a comparison.

Table I. Calculated temperatures for various configurations of the two can container

Surface	Container # 1 in iar, P=1 W		Container # 2 on the rack with gap, P=10.35 W		Container # 3 on the rack without gap, P= 10.35 W	
	Our predictions, ^{0}C	Calculations [3], ^{0}C	Our predictions, ^{0}C	Calculations [3], ^{0}C	Our predictions, ^{0}C	Calculations [3], ^{0}C
1. Outer can top	40.2	41.1	32.5	40.0	28.9	35.7
2. Outer can side	42.0	42.3	34.3	38.9	31.8	36.0
3. Inner can top	47.2	47.3	47.3	55.6	41.9	45.6
4. Inner can side	43.0	42.8	37.0	41.7	40.0	37.8
5. Pu ingot top	58.7	60.0	73.2	89.0	63.6	67.5
6. Pu ingot side	58.6	60.0	72.0	88.0	61.8	65.6
7. Rack bottom	-	-	35.4	56.7	51.9	60.6

Analysis of the data presented in Table I shows the following. For the first configuration with heat-generation 1 W a very good agreement was obtained between our results and data from [2] – the difference is low than 1.5 ^{0}C. The same mathematical model has been employed both in our predictions and calculations [2]. Essential discrepancies with data [3] for configurations of the container with heat-generation of 10.35 W can be explained by usage of different models. In our predictions the temperature filed in the container has been calculated taking into account free convection of air in gaps whereas in work [2] calculations have been done with immobile air using effective, calculated early from other configurations thermal coefficients. Moreover, boundary conditions in our predictions were specified as the heat transfer into environment governed by the Newton law (instead of the power relation [2]) with large enough heat transfer coefficient that, as a whole, resulted in more low values of the temperature.

3.2 MODELING OF CONTAINER AT400R

For container AT400R [3] verification predictions of two thermal regimes provided by experimental data have been done – the steady-state thermal regime for the container with the internal heat source and transient heating of the container under the condition of the prescribed fire. A complicated composite structure of the container consisted of several materials was taken into account. Air convection in gaps was not considered due to their small

sizes. A good agreement between our predictions and measurements of the temperature in specified points has been obtained in both cases. Calculated results for steady-state thermal regime in container AT400R appearing from the internal heat source of power 20 W are presented in Table II. For a comparison there are also shown experimental data from work [3]. A good enough agreement was obtained between calculations and measurements. The maximal difference is about 5^0C and takes place at the container lid whereas in other points it is less than 3^0C. The presented calculations can be treated as the validation of code LMN2D.

Table II. Predicted and experimental data for container AT400R

Container element	Prediction, ^{0}C	Experiment [3], ^{0}C
Model	83.0	81.7
Closing plate	81.0	78.3
Side surface of internal vessel	63.2	65.0
Container lid	47.3	42.2
Container bottom	38.4	41.7
Container side surface	38.0	40.6

The container behavior under the condition of a fire has been calculated, too. The impact of the fire on the container was given via the taken from experiments varying in time value of the temperature on its boundaries. The initial temperature of the container was 70 ^{0}C, duration of the fire – 300 min. Figure 1 shows variation in time of the temperature at points 1, 2 and 3, located on the external steel vessel of the container (see detailed positions of these points in [3]). All curves are very close one to another and practically coincide with the specified temperature of the fire.

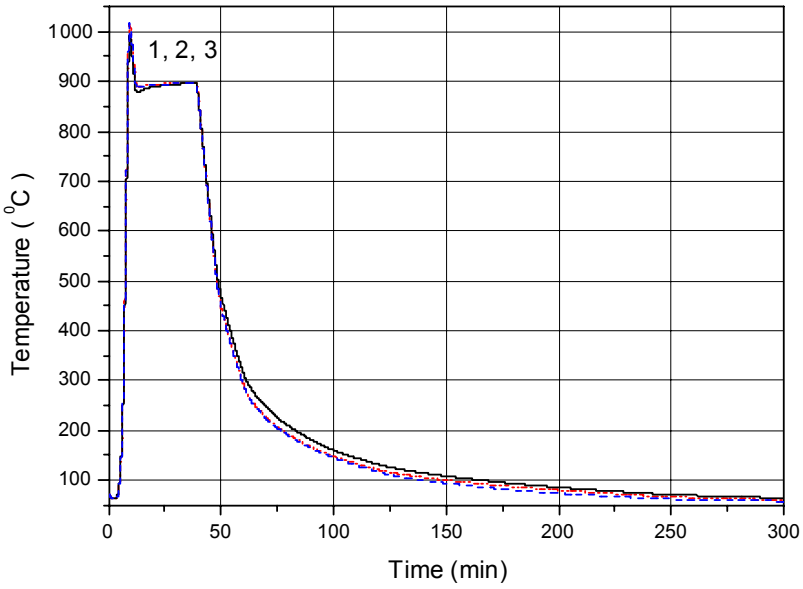

Figure 1. Temperature at points 1, 2 and 3 vs time.

In Figure 2 there is shown variation in time of the temperature at points 5, 6 and 7, located, respectively, on the side surface of the internal vessel at midpoint (point 5) and in the upper its part (points 6 and 7). Calculated curves are in good enough agreement with experimental data from [3].

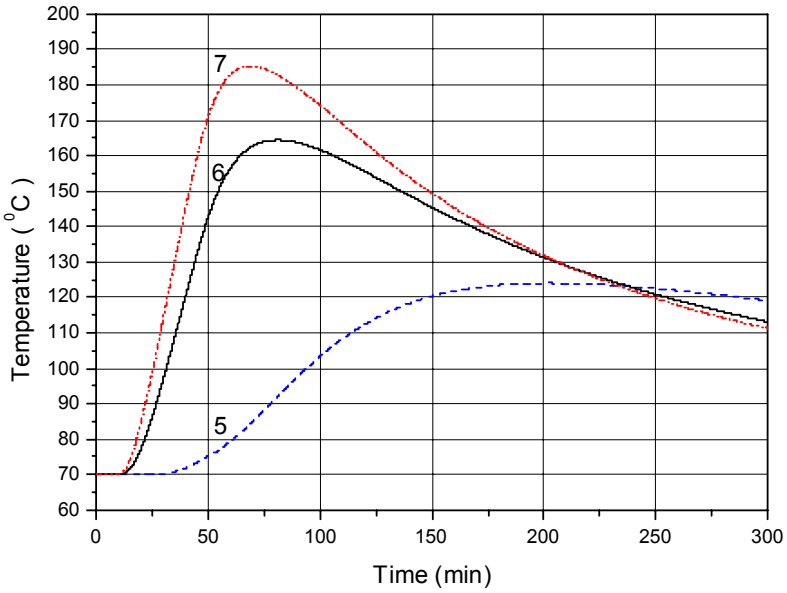

Figure 2. Temperature at points 5, 6 and 7 vs time.

Calculated curves are in good enough agreement with experimental data from [3].

ACKNOWLEDGEMENTES

This work was supported by Grant № 00-01-00290 of Russian Foundation of Fundamental Researches and by Project # 1449-01 of International Scientific Technology Center.

REFERENCES

1. IAEA, "Safe Handling and Storage of Plutonium," *Safety Reports*, series № 9, Austria, September (1998).
2. S. J. Hensel, S.Y. Lee, J. B. Schaade, "Plutonium storage Thermal Analysis," *Westinghouse Savannah River Co*., WSRC-MS-97-0002.
3. "AT-400R Compliance Test Report," **Vol. 1-4**, *Sandia National Labs*., Albuquerque (1995).
4. S. Stevkovski, D. L. James, "Thermal Analysis of Plutonium storage containers," *Proceedings of Nineteen ninety-(1999) researcher's conference*, Amarillo College Business and Industry Center, Amarillo, TX(U.S.A), July 19-21, pp. 13-16 (1999).
5. T. D. Knight, R. G. Steinke, "Thermal Analyses of Plutonium Materials in Stainless Steel Containers," *Transaction of ANS*, **Vol. 77**, pp.144-145.

6. "Join U.S./Russian Plutonium Disposition Study. Long-term storage of fissile material." July (1999).
7. E.S. Oran, J.P. Boris, *Numerical Simulation of Reactive Flow*, Elsevier, New York, (1987).
8. Yu.V. Lapin, M.Kh. Streletz, *Internal Flows of Gas Mixtures*, Nauka, Moscow, (1989) (in Russian).
9. P.J. O'Rourke, F.V. Bracco, "Two scaling transformations for the numerical computation of multidimensional unsteady laminar flames," *Journal of Computational Physics*, **Vol. 33**, pp.185-203 (1979).
10. A. Majda, J. Sethian, "The derivation and numerical solution of the equations for zero-Mach number combustion," *Combust. Sci. Tech.*, **Vol. 42**, pp.185-205 (1985).
11. E.P. Visser, C.R. Kleijn, C.A.M. Govers et al., "Return flows in horizontal MOCVD reactors studied with the use of TiO2 particle injection and numerical calculations," *J. Crystal Growth*, **Vol. 94**, pp.929-946 (1989).
12. M. Buffat, "Simulation of two- and three-dimensional internal subsonic flows using a finite element method," *Int. J. Numer. Methods Fluids*, **Vol. 12**, pp.683-704 (1991).
13. S.V. Patankar, *Numerical Heat Transfer and Fluid Flow*, Hemisphere, Washington, D.C. (1980).
14. A.N. Pavlov, A.A. Ionkin, A.V. Voronkov, A.G. Churbanov, "A homogeneous algorithm for calculation of heat and mass transfer in domains of complicated structure," KIAM RAS, *Preprint # 8* (1998) (in Russian).